euspen's 26th International Conference & Exhibition, Krakow, PL, June 2026

www.euspen.eu

Productivity enhancement and burr reduction in Ti6Al4V single lip microdrilling using ultrasonic vibration assistance

Bernie Cheruiyot*, Richard Börner, Andreas Nestler, Andreas Schubert

Professorship Micromanufacturing Technology, Chemnitz University of Technology, Reichenhainer Str. 70 09126 Chemnitz, Germany

kiplelgo@proton.me

Abstract

Mechanical microdrilling is a critical process in advanced manufacturing of high-precision components, such as in medical and aerospace industries. However, the process is limited by low tool stiffness, poor chip removal and significant burr formation. Ultrasonic assistance is proposed to overcome some of these challenges, converting the continuous cutting process into an intermittent one. Some of these benefits are the support of chip breaking and reduced friction between the tool and the bore wall. This research evaluates the effectiveness of ultrasonic assistance in single flute microdrilling of Ti6Al4V alloy. Experiments were conducted for a diameter of 1 mm at feeds of 2 µm and 4 µm, both with and without ultrasonic assistance. Results demonstrate that while the tool is broken at 4 µm feed in regular drilling, the process is technically feasible with ultrasonic assistance, effectively halving the drilling time per hole. Additionally, the ultrasonically assisted process shows improvements in chip formation, burr reduction and process stability.

Microdrilling, single flute drill, Ti6Al4V, ultrasonic vibration assistance

1. Introduction

Micro-holes (diameter < 1 mm) are a critical feature in high precision applications. These include microscopic nozzles in fuel injectors for combustion engines [1] and aerospace cooling channels for turbine engines [2]. Microdrilling is also useful for orthopaedic implants such as intramedullary nails, as research done on mice in veterinary medicine shows [3]. Mechanical microdrilling is preferred in many applications of medical manufacturing for achieving high hole straightness and surface quality. Additionally, drilling avoids formation of a chemically altered heat-affected zones and microcracks that may arise from thermal ablation methods such as electro-discharge machining (EDM) and laser drilling [4]. This is especially important for medical materials such as Ti6Al4V, which is preferred for medical applications due to its corrosion resistance, high strength, low weight and biocompatibility [5]. At a micro-scale, drilling suffers problems such as low tool stiffness, chip entanglement and high burr formation [4]. The material removal mechanism shifts to forming due to very low undeformed chip thickness in the same order of magnitude as the cutting edge radius, where material is pushed away and formed rather than cut into a chip [6]. This increases the specific energy required for material removal. Ti6Al4V exhibits characteristics that make it difficult to process, such as a high specific strength and resistance to thermal softening [7]. Single flute gun drills are a special drill geometry particularly suitable to microdrilling, with higher stiffness due to a greater cross-sectional area, and internal coolant delivery incorporated into their design. They are typically used at lower feeds than twist drills. High-pressure internal coolant (80 bar – 120 bar) is essential for their application [8]. Pressure values are dependent on drill diameter and hole aspect ratio, with tool manufacturers usually providing a guide to the pressure setting. Ultrasonic (US) assistance has been explored as an enhancement to mechanical microdrilling, transforming the cutting into an intermittent process [9]. This leads to benefits such as better chip formation and minimal burr formation [4]. This research aims to extend the productivity of single flute microdrills by increasing the viable feed as well as reduce burrs at the hole exit by leveraging the benefits of US assistance. These outcomes are to be validated experimentally.

2. Methodology

Conventional mechanical microdrilling has two main motions of the tool: the feed of the tool into the workpiece, as well as the rotation of the tool about its axis. US assistance introduces a third motion, the oscillation of the tool along its axis, occurring at ultrasonic frequencies. The cutting is thus transformed from a continuous chip formation process to an intermittent process, subject to the process parameters falling within a specific operating window and combination with each other. The intermittent contact between the tool and workpiece results in more steady thrust and cutting forces, as well as smaller, more manageable chips. Chip breaking is promoted by the varying undeformed chip thickness and intermittence of cutting. These benefits create the possibility to extend the productivity and enhance the stability of mechanical drilling using this technique.

2.1. Kinematics of ultrasonic-assisted drilling

The kinematics of the drill bit can be modelled mathematically by taking into consideration the linear feed movement and rotation of the tool, as well as the ultrasonic oscillations. The z-, x- and y-axis positions of a point on the circumference of the tool as seen in Figure 1 can be determined as follows:

$$z = -f \times n \times t + A \times sin(2\pi f_{\mathrm{US}} t) \quad \text{Eq 2.1}$$

$$x = r \times cos\,\theta \quad \text{Eq 2.2}$$

$$y = r \times sin\,\theta \quad \text{Eq 2.3}$$

A represents the amplitude of oscillations, i.e. half of the peak-to-peak displacement, f_{US} is the frequency of ultrasonic oscillation and *r* is the radius of the tool. The feed is given by *f*, representing the feed per revolution, which in the case of single flute drills is equivalent to the feed per tooth. The rotational speed is given by n and t represents the time. The tool path can be mathematically plotted in 3D space as shown in Figure 1, showing the path of a single point on the tool circumference.

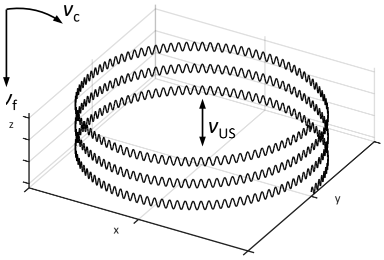

Figure 1. Path of a point on the outer cutting edge. v_f represents the feed velocity, v_{US} represents velocity due to ultrasonic oscillation and v_c represents the cutting speed.

To ensure that the intermittent cutting is attained, the feed velocity must be less than the maximum instantaneous velocity of the oscillating tool (critical velocity). The critical velocity is determined by the ultrasonic parameters amplitude and frequency. Intermittent cutting is only attained if the feed velocity is lower than the critical velocity. Following the previously described model, this relation is specifically constrained to a point on the tool periphery.

2.2. Experimental parameters and instrumentation

Experiments were designed to isolate the effects of feed and ultrasonic amplitude. The first experiment was conducted to establish a baseline of the machining performance and characteristics as recommended by the tool manufacturer. Subsequently, the effectiveness of US assistance and its benefits were evaluated. This was followed by testing the possibility of US assistance extending productivity levels beyond the standard recommended parameters. Table 1 shows the machining and US parameters used for the experiments.

Table 1. Experimental parameters

Test	Feed/ µm	Peak-peak US amplitude / µm	Holes drilled
Ref2	2	0	100
US2	2	3	100
Ref4	4	0	22
US4	4	3	550

The spindle speed was kept constant at 9550 1/min, corresponding to a cutting speed of 30 m/min for the 1 mm drill bit used. An internal coolant pressure was set to 40 bar, the maximum for the KERN Pyramid Nano machining centre applied. Although this pressure is below the minimum recommended pressure due to machine limitations, the setup can be used as a test case for extending the functionality of existing systems with limited capabilities. A botek Type 113 single flute cemented carbide drill with a TiAlN coating was used, with a drill-point angle of 110° and drill body length of 62 mm. US oscillations were induced by a VibroCut Precision Line oscillator, fitted with a 6 mm shrink fit chuck for the drilling tool, which was set to its minimum power level. The resulting peak-to-peak amplitude of 3 µm (A_{pp}) was applied for the experiments. The specimen used in this experiment was a 12 mm thick Ti6Al4V disc with a diameter of 70 mm, onto which a rectangular pattern of holes was drilled. As single flute drills are asymmetrical and not inherently capable of self-centering, the specimen was pre-piloted with holes of 1.01 mm diameter using a botek Type 153 pilot drill with a drill-point angle of 140° to a depth of 2.5 mm, followed by drilling through the whole depth of the specimen. The single flute drill was initially fed into the pilot holes at a lower spindle speed of 50 1/min to aid the location of the hole and then spun up to the operational spindle speed. The experimental setup used is shown in Figure 2.

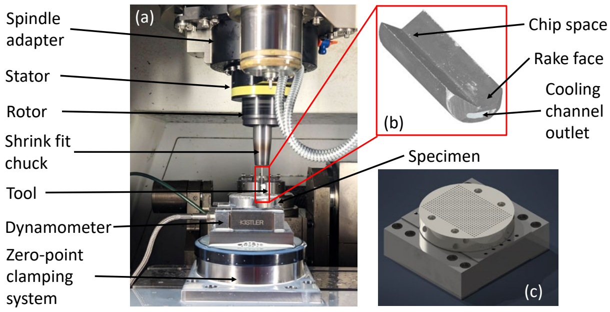

Figure 2. The experimental setup used, showing (a) the setup in the machining centre, (b) 3D scan of the tool and (c) 3D construction of the mounted and pre-piloted specimen.

2.3. Evaluation and process characterisation

Axial and lateral forces were measured using a dynamometer, onto which the test specimens were mounted, at a sampling frequency of 1 kHz. The raw force signal was evaluated using a custom MATLAB script to isolate the data for individual holes, enabling the calculation of mean forces and standard deviations on a per-hole basis. The z-direction signal is a measure of the thrust force, which is of primary interest in this investigation. RMS values were calculated for forces in x-direction in order to capture both positive and negative values generated by the rotating tool during drilling.

Intermediate micrographs of the tool were taken at fixed intervals to monitor the progression of tool wear as well as their operability. Chips collected from each experiment were analysed using both a Keyence digital light microscope as well as a scanning electron microscope (SEM) to characterise their shape and dimensions.

3. Results

3.1. Baseline experiment – Feed of 2 µm

The initial experimentation focused on establishing a process baseline and validating the process feasibility. A target of 100 holes drilled was successfully achieved using the maximum recommended feed of 2 µm. The thrust forces in this experiment were considerably low, with a starting value of 4.8 N and rising to a maximum of 11.2 N. This progression can be seen in Figure 3. Error bars are added to every fifth hole to enhance readability, showing the standard deviation of the thrust forces.

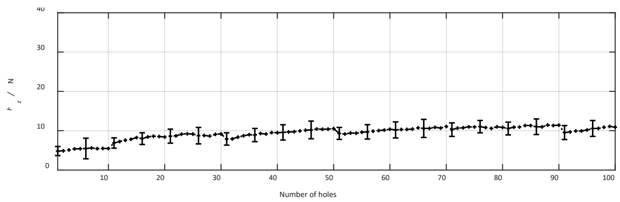

Figure 3. Thrust forces in reference experiment, 2 µm.

Introduction of US oscillations results in both a higher magnitude of forces, as well as greater dispersion. The standard deviation rises from a maximum of 3.0 N to 7.5 N. The average force is only marginally increased, starting at 8.1 N and rising to a maximum of 13.8 N. This is a smaller increase compared to the reference experiment for the same number of holes drilled. The progression of forces in this experiment can be seen in Figure 4.

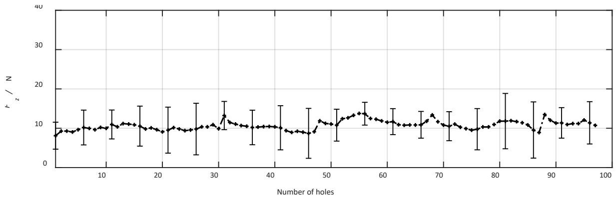

Figure 4. Mean thrust force using US assistance with feed of 2 µm.

The forces in x-direction in the reference experiments were also very low, with a grand mean RMS value of 0.19 N and within a narrow force envelope. This is due to the low chip load caused by the small feed, requiring less energy to form the chip. There is a more noticeable difference in the lateral forces with the additional of US assistance, with an average $F_{x,RMS}$ of 1.15 N, an increase of about 500 %. These forces are considerably low, with no tool chatter that would indicate imminent tool failure.

Tool wear is slightly worse using US assistance, which can be attributed to the repeated hammering of the cutting edge in the workpiece. A side-by-side comparison of the tool rake face is as shown in Figure 5, where the increased wear of the inner cutting edge can be seen in Figure 5 (b).

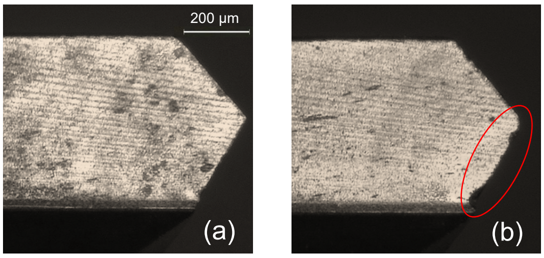

Figure 5. Side-by-side comparison of tool rake face at 2 µm after 60 holes (a) without US assistance and (b) with US assistance.

3.2. Experiments with increased feed of 4 µm

The initial test conducted at 4 µm feed without US assistance yielded only twenty-two holes before the tool irretrievably broke. This was taken as an indicator of technical infeasibility, as 4 µm is double the maximum recommended feed. However, a subsequent test with US assistance was successful. The mean forces in this experiment were considerably higher than at 2 µm feed, reaching a peak mean of 25.8 N with a grand mean of 19.0 N. Dispersion also increased, with an average standard deviation of 8.4 N. The progression of the forces through the 100-hole sequence with US assistance is as shown in Figure 6.

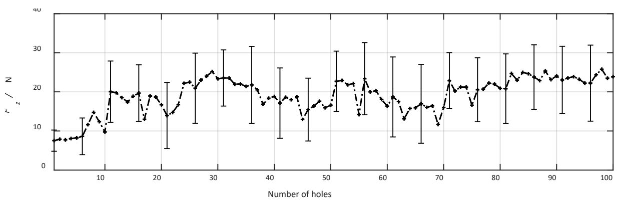

Figure 6. Mean thrust forces using US assistance with feed of 4 µm.

The force signal was observed to show two zones, an initial low and stable zone, followed by a second zone with higher magnitude and greater signal dispersion. This is attributable to the friction inside the hole walls that causes the tool to stick, increasing the thrust force required to maintain the set feed. A representative force signal from a sample hole in this experiment is shown in Figure 7, with the portion of the signal from the tool engagement point to hole exit marked.

The lateral forces in this experiment showed a falling trend that roughly corresponds to the magnitude of thrust force. The magnitude of forces (RMS) was higher than the previous experiments, with a minimum RMS of 1.0 N, maximum RMS of 2.4 N and a grand RMS mean of 1.6 N. This is a modest increase compared to the experiment conducted at 2 µm which does not linearly correspond to feed being doubled. However, the drilling time per hole is halved.

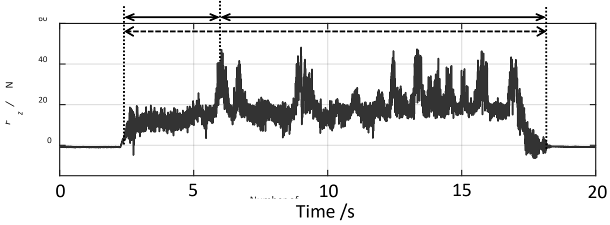

Figure 7. Representative force signal of a hole drilled at 4 µm showing the two-zone progression of thrust force as the hole is drilled

The tool used in this experiment showed the greatest extent of wear both on the cutting edge as well as at the tool tip. This is expected as the tool is subject to the greatest stress, with a higher chip load in addition to the ultrasonic hammering. The process is, however, free from chatter and other indications that the tool may be under excessive stress. Figure 8 shows the damage on the cutting edge of the tool.

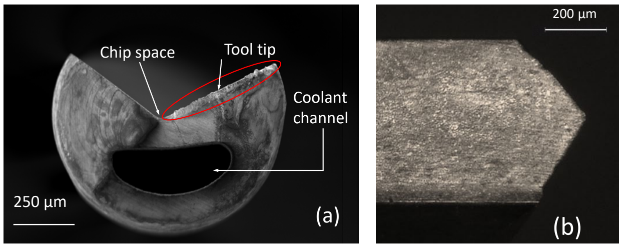

Figure 8. Tool wear after 500 holes represented by (a) SEM image of the tool tip and cutting edge and (b) rake face image.

3.3. Endurance test – 4 µm

The same parameters were used to further test the robustness of the system, and a total of 500 holes were drilled before the experiment was concluded. During this endurance test, the forces remain stable within a narrow window with no significant increasing trend. The thrust forces show a peak value of 25.8 N, with a grand mean value of 19.0 N and a standard deviation of 8.4 N. Thus, the process with US assistance is a viable choice for serial production, particularly considering that the regular test conducted without US assistance resulted in a broken tool. The trend of thrust force is shown in Figure 9.

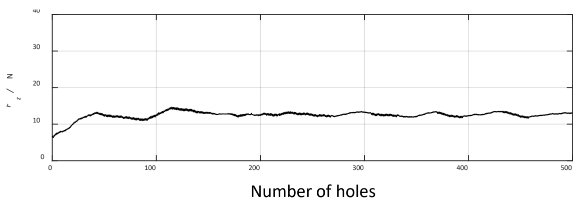

Figure 9. Force progression (rolling mean) in endurance test, 4 µm.

3.4. Formation and reduction of burr

An additional problem with microdrilling is the formation of high exit burrs. At the bottom of the drilled hole, just before the drill exits the workpiece, the thin layer of material left is formed into a burr rather than being removed cleanly by cutting. This problem is exacerbated at high feeds, as the final layer is thicker and results in a larger burr. US assistance may help in reducing the burr, as the high impact of the oscillating tool results in a clean cut. The analysis of burr formation was done by classifying the burrs into three categories: nearly no burr formation (Category 0), various formations of a burr around the hole circumference (Category 1), and the formation of a drill cap (Category 2). Sample SEM micrographs of the burr types observed, which were taken from the through-hole exit side, are shown in Figure 10.

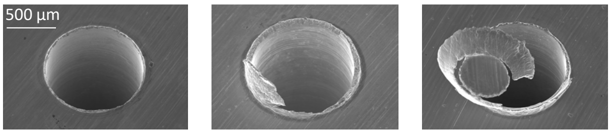

Category 0 Category 1 Category 2

Figure 10. The burr classification categories at the hole exit.

The classification data confirms that occurrence of burr formation is increased at a higher feed. At 4 µm feed, 99 % of holes drilled have a burr. Burr sizes were also higher, with over 50 % of holes drilled exhibiting a drill cap.

As the frequency of burr formation and burr size is reduced at a lower feed, a machining strategy was conceptualised to minimise the formation of burrs. This involved drilling at a compound feed, beginning at 4 µm as had been previously done. The feed was then lowered to 1 µm for the last 500 µm. A test was conducted on a fifty-hole sequence using the same drilling tool as for the ultrasonic test at 4 µm up to 500 holes. Of these, a drill cap was formed in twelve holes, while the remaining thirty-eight were nearly burr-free, representing a 76 % rate of nearly burr-free drilling. This shows that the use of a compound feed can be an effective strategy in reducing burr formation. Crucially, the drilling time is not significantly increased, with the compound feed strategy requiring about 17 s compared to 14.5 s using a constant 4 µm feed. This benefit would be even greater for deep drilling, as a much larger proportion of the hole is drilled faster at the higher feed. The distribution of burrs formed in each category grouped by experiment is shown in Figure 11. The label 'US4*' represents the burr reduction test.

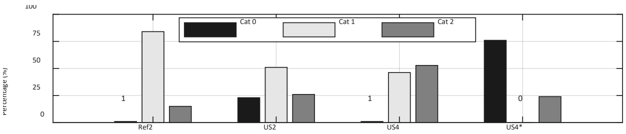

Figure 11. Distribution of burr formation by type.

3.5. Chip formation and morphology

The chips formed in the experiments were also observed by SEM, revealing differences in their size and morphology. The chips formed at 2 µm feed without US assistance were the longest, exhibiting a conical shape with several cracks formed. Addition of ultrasonic vibrations promoted chip breaking through the intermittent cutting and a varied undeformed chip thickness, resulting in considerably smaller and more broken chips. On further raising the feed to 4 µm, the chips are slightly larger in size but are still broken into smaller particles. The chips formed in the three experiments can be seen in representative samples shown in Figure 12. All micrographs were taken with the same magnification.

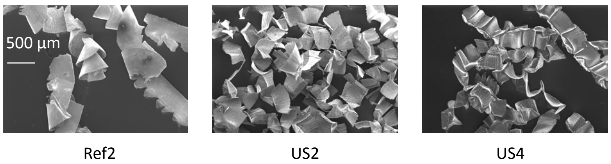

Ref2 US2 US4

Figure 12. Chip micrographs from the microdrilling experiments.

4. Summary and conclusions

The potential of US assistance in microdrilling is confirmed for Ti6Al4V in this study. A higher feed than is feasible under regular drilling conditions is made possible using US assistance. The result is a stable and robust process suitable for continuous operation. Notably, the compound feed machining strategy yields a nearly burr-free result, while chip fragmentation is aided by the US oscillations to improve evacuation and avoid clogging. The maximum feasible feed for these single flute micro drills is doubled from 2 µm to 4 µm, halving the drilling time without causing premature tool failure. This was validated in the 500-hole sequence. US assistance effectively mitigates some of the micro-scale effects such as chip forming due to a very low chip load, transitioning the material removal mechanism towards a more stable intermittent cutting process. This is an important improvement to the mechanical microdrilling process using single flute micro-drills. It enables serial production of parts that are required in high quantities, such as medical implants and orthopaedic fixtures which are required in high quantities and disposable for hygienic reasons.

Further research should establish the operational limits of US assistance in mechanical microdrilling. As the current process parameters already achieve clear tool-workpiece separation, further raising the ultrasonic amplitude may yield diminishing returns while increasing the impact energy on the tool edge, potentially accelerating tool wear by chipping. In addition, critical feeds should be defined, where the intermittent cut is maintained with high process stability. Other difficult-to-machine materials, such as nickel-based superalloys, may also benefit from this technique, allowing broader industrial application.

References

[1] H. Yu, G. Chen, J. Xu, J. Wang, Z. Yu and X. Tang, "An Experimental Study of Ultrasonic Assisted Micro-Holes Drilling," in *2018 IEEE Int. Conf. on Manipulation, Manufacturing and Measurement on the Nanoscale (3M-NANO)*, 2018.

[2] L. Subasi, M. I. Gokler and U. Yaman, "A process modeling approach for micro drilling of aerospace alloys with a waterjet guided laser system," *Optics & Laser Technology,* vol. 148, p. 107682, April 2022.

[3] T. Histing, M. D. Menger, T. Pohlemann, R. Matthys, T. Fritz, P. Garcia and M. Klein, "An Intramedullary Locking Nail for Standardized Fixation of Femur Osteotomies to Analyze Normal and Defective Bone Healing in Mice," *J. of Visualized Experiments : JoVE,* p. 54472, November 2016.

[4] M. Hasan, J. Zhao and Z. Jiang, "A review of modern advancements in micro drilling techniques," *J. of Manuf. Processes,* vol. 29, p. 343–375, October 2017.

[5] E. Marin and A. Lanzutti, "Biomedical Applications of Titanium Alloys: A Comprehensive Review," *Materials,* vol. 17, p. 114, January 2024.

[6] X. Huang, F. Jiang, Z. Wang, X. Wu, S. Huang, Y. Liu, J. Zhang and X. Shi, "A review on the balancing design of micro drills," *Int. J. of Advanced Manuf. Tech.,* vol. 126, p. 4849–4871, June 2023.

[7] G. Gao, Z. Yuan, Z. Xia, Z. Fu, D. Xiang and B. Zhao, "Study on thrust force of ultrasonic-assisted vibration micro-hole drilling of titanium alloy," *The Int. J. of Advanced Manufacturing Tech.,* vol. 112, p. 3399–3413, January 2021.

[8] E. Oezkaya, A. Baumann, S. Michel, D. Schnabel, P. Eberhard and D. Biermann, "Cutting fluid behavior under consideration of chip formation during micro single-lip deep hole drilling of Inconel 718," *Int. J. of Modelling and Simulation,* vol. 43, p. 49–63, March 2023.

[9] S. Ullah, Z. Liang, Y. Ma, Y. Du, Z. Su, Z. Yin, L. Xiong, M. U. Rehman, K. Pattamaporn and T. Zhou, "State-of-the-art review on ultrasonic vibration-assisted micro-drilling," *The Int. J. of Advanced Manufacturing Tech.,* vol. 138, p. 4935–4963, June 2025.